Polymer Journal
https://doi.org/10.1038/s41428-025-01132-7

ORIGINAL ARTICLE

Self-assembled nanogels from polysaccharides grafted with short oligonucleotides: control of size and thermoresponsiveness

Shin-ichi Sawada[1] · Hirokazu Iwamoto[2] · Yoshihiro Sasaki[2] · Kazunari Akiyoshi[3]

Received: 17 October 2025 / Revised: 12 November 2025 / Accepted: 13 November 2025

Abstract

Pullulan, a water-soluble polysaccharide, was grafted with short (4-mer and 6-mer) oligonucleotides containing bridged nucleic acids (BNAs) to produce self-assembled nanogels through the formation of oligonucleotide double chains. Dynamic light scattering measurements and transmission electron microscopy images revealed that oligonucleotide-grafted pullulans containing oligonucleotides with different chain lengths, sequences, and numbers of BNA substituents in water formed nanogels and that their aggregation behavior changed with temperature. Gel electrophoresis revealed that the complexation of fluorescently labeled oligonucleotides with these nanogels was possible, and flow cytometry measurements indicated that the cellular uptake of oligonucleotides was significantly enhanced when the oligonucleotides were complexed with the nanogels. Therefore, self-assembled nanogels derived from oligonucleotide-grafted polysaccharides can be applied as carriers of nucleic acids and nucleic acid-conjugated molecules for intracellular delivery.

Introduction

Self-assembled materials constructed from polymers through noncovalent interactions, such as hydrophobic and electrostatic interactions, have been extensively studied in various fields [1–3]. Among them, self-assembled nano-sized gel particles are prevalent in the fields of biotechnology and medicine [4–6]. We developed nanogels using cholesterol group-grafted pullulan (CHP) that self-assembled in water through nanoaggregation on the basis of hydrophobic interactions [7, 8]. CHP-based nanogels can trap proteins inside their network and show chaperone-like activity. They have been widely applied as nanocarriers of biopharmaceutical agents, especially for cancer and nasal vaccines [8, 9]. As the basis of self-assembled nanogels, polysaccharides are not only pullulan with a linear structure but also complex molecules with various structures and functions, such as mannan, branched glycogen, dextrin, and cycloamylose [7, 8, 10]. Various self-assembled nanogels have been constructed from water-soluble polymers by introducing self-assembling units that participate in electrostatic interactions, host–guest interactions, and dynamic covalent bonding [7, 8].

Stimuli-responsive nanogels undergo structural changes, including volume phase transitions, in response to external stimuli [2, 11, 12]. They include photoresponsive, pH-degradable, temperature-responsive, and redox-responsive nanogels. These properties make stimuli-responsive nanogels suitable for various medical applications [13–15].

Gel materials that self-assemble through the formation of nucleic acid duplexes are also responsive to various stimuli. These gel materials are constructed using nucleic acids as the only component [16–18]. However, in recent years, functional gel materials consisting of synthetic polymers modified with nucleic acids [18], such as nanogels using DNA aptamers to cross-link with specific proteins [19] and nanogels that use siRNA as both a biologically active agent and a cross-linking agent [20], have increasingly been

Supplementary information The online version contains supplementary material available at https://doi.org/10.1038/s41428-025-01132-7.

✉ Shin-ichi Sawada
shsawada@chiba-u.jp

✉ Kazunari Akiyoshi
akiyoshi.kazunari.2e@kyoto-u.ac.jp

[1] Synergy Institute for Futuristic Mucosal Vaccine Research and Development, Chiba University, Chiba-shi, Chiba, Japan

[2] Department of Polymer Chemistry, Graduate School of Engineering, Kyoto University, Kyoto, Japan

[3] Department of Immunology, Graduate School of Medicine, Kyoto University, Kyoto, Japan

Published online: 28 January 2026

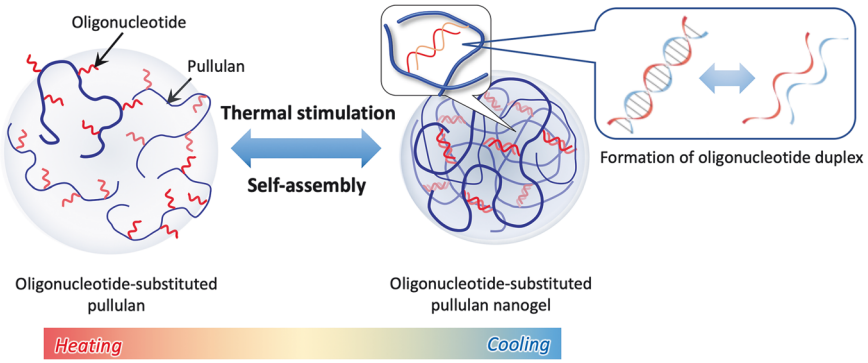

Fig. 1 Schematic illustration of the formation of oligonucleotide-grafted pullulan nanogels

reported. In addition, macrogels that recognize DNA targets and undergo volume phase transitions [21] and oligonucleic acid-modified hydrogels that respond to visible and ultraviolet light for actuator applications have been reported [22].

The double strands of nucleic acids stabilized by hydrogen bonds show temperature-dependent binding and dissociation characteristics. However, when oligonucleotides are used as self-assembling units, chains longer than 20 mer are generally required for stable double-strand formation under physiological conditions. In this study, we focused on the possibility of forming stable duplexes with very short chain lengths by incorporating bridged nucleic acids (BNAs), which are artificial nucleic acids. In general, the sugar residues of naturally occurring nucleic acids are in the S-type (C2'-*endo*) conformation and form B-type helical structures during duplex formation. In contrast, 2',4'-BNA^{NC} (2'-*O*,4'-*C*-aminomethylene-bridged nucleic acid), a bridged artificial nucleic acid developed by Imanishi et al. and incorporated into DNA, promotes the formation of an A-type helix because its sugar residue is fixed in an N-type conformation [23]. Compared with the B-type helix structure, the A-type helix structure of the DNA duplex is reported to have stronger stacking interactions, and ΔH favors duplex formation. As a result, stable duplexes from short chains of oligonucleic acids with high T_m are possible when 2',4'-BNA^{NC} is incorporated. Various derivatives of BNA, such as 2',4'-BNA, 3'- or 5'-amino-2',4'- BNA, and 2',4'-BNA^{COC}, have been reported. In this study, we used 2',4'-BNA^{NC}, which is highly resistant to degrading enzymes and has been developed as an antisense drug [24].

Herein, we report new self-assembled nanogels produced through the formation of double strands of short oligonucleotides serving as self-assembling units. To prepare thermoresponsive small nanogels of less than 100 nm, we designed oligonucleotides that could form stable duplexes of short chain lengths using 2',4'-BNA^{NC}. The introduction of BNAs to oligonucleotides (4-mer or 6-mer) drastically increased the T_m of the molecule. Therefore, we synthesized new self-assembling polysaccharides (pullulan) by grafting short oligonucleotides containing BNAs (with approximately 2 units of oligonucleotides per 100 monosaccharides) and investigated the self-assembly of thermoresponsive nanogels through the formation of double-stranded oligonucleotides (Fig. 1). The effects of the sequence, chain length, and number of BNAs in the oligonucleotides on the properties of the self-assembled polymers were investigated. We also evaluated the potential application of the nanogels as carriers of nucleic acids or nucleic acid-conjugated molecules.

Materials and methods

Synthesis of BNA-modified oligonucleotides

All reactions were performed under an atmosphere of nitrogen or argon. Unless otherwise indicated, all the chemicals from commercial sources were used without further purification. 2',4'-BNA^{NC}(N-Pac)-G^{iBu}-phosphoamidite and 2',4'-BNA^{NC}(N-Pac)-^{m}C^{Bz}-phosphoamidite were obtained from BNA (Osaka, Japan). The primers used to support 5 G 350 (A, T, and C) were purchased from GE Healthcare (NY, USA). 5'-Hexynyl-phosphoramidite, dA-CE-phosphoramidite, dT-CE-phosphoramidite, dC-CE-phosphoramidite, deblocking solution (3% trichloroacetic acid in dichloromethane (CH_2Cl_2)), Cap A (tetrahydrofuran (THF), 1,2,6-lutidine, and acetic anhydride mixture), Cap B (16% 1-methylimidazole in THF), and oxidizing solution (0.02 M iodine in THF) were obtained from Glen Research (VA, USA). 5-Ethylthio-1H-tetrazole (ETT, 0.45 M) in anhydrous acetonitrile (MeCN), superdehydrated MeCN, and an ammonia solution were obtained from Wako Pure Chemical (Osaka, Japan). Superdehydrated MeCN was dried in a molecular sieve prior to use. Proton nuclear magnetic resonance (^{1}H NMR) (400 MHz) spectra were recorded on an AVANCE III spectrometer (Bruker, MA, USA). Chemical shifts are reported in parts per million downfield from

tetramethylsilane or a deuterated solvent as the internal standard. Mass spectra were measured on an Exactive Plus (Thermo Fisher Scientific, MA, USA) or Ultraflex III (Bruker, MA, USA) mass spectrometer.

Oligonucleotide synthesis

Manual synthesis of oligonucleotides was performed on the 40 µmol scale using a gas-tight syringe with ETT as the activator following a standard phosphoramidite protocol. Briefly, superdehydrated MeCN, deblocking solution, Cap A solution, Cap B solution, and oxidizing solution were dispensed into ampules in a glove box and tightly sealed. Next, the primer support 5 G (solid phase support) was placed in a gas-tight syringe, washed five times with 3 mL of superdehydrated MeCN, and then dried under reduced pressure. After drying, 2 mL of deblocking solution was injected into the reaction vessel, and treatment to remove dimethoxytrityl (DMT) was performed for 2 min. This procedure was repeated five times to completely remove DMT, followed by washing with ultradesiccated MeCN and drying under reduced pressure. Next, the phosphoramidite solution dissolved in 2 mL of 0.45 M ETT solution was placed in a gas-tight syringe for the coupling reaction, which took 30 min. Then, the reaction mixture was washed with acetonitrile and dried under reduced pressure. Cap A (2 mL) and Cap B (2 mL) were added to the gas-tight syringe and allowed to react for 3 min. After being washed with acetonitrile and dried under reduced pressure, 5 mL of oxidizing solution was added, and the oxidation reaction was carried out for 10 min, followed by washing and drying. This process was repeated to synthesize oligonucleotides of the target sequence, and finally, 5'-hexynyl-phosphoramidite was coupled. After synthesis, 28% ammonia solution was added for 1 h to cleave the oligonucleotides from the support, and the reaction mixture was maintained at 55 °C for 24 h. The ammonia solutions were then concentrated, and the crude oligonucleotides were purified using reversed-phase high-performance liquid chromatography (RP-HPLC) with a COSMOSIL $5C_{18}$-AR-II (10 mm ID × 150 mm or 6.0 mm ID × 150 mm) packed column (Nacalai Tesque, Kyoto, Japan) using 5–50% MeCN in 0.1 M triethylammonium acetate buffer (pH 7.0). The oligonucleotides were characterized by mass spectrometry, and their purity was analyzed by HPLC.

Melting temperature (T_m) measurements

Ultraviolet (UV) absorbance melting curves were acquired by recording the absorbance at 260 nm with respect to the increase in temperature (0.5 °C/min) using a UV-1650 UV–visible spectrophotometer (Shimadzu Corp., Kyoto, Japan) equipped with a Peltier temperature controller. T_m values were determined from the maximum value of the first derivative of the melting curve. The samples were annealed by decreasing the temperature from 90 °C to 4 °C at a rate of 0.5 °C/min.

Synthesis of oligonucleotide-grafted pullulan

All the solvents were reagent grade, were purchased from commercial sources, and were used without further purification. 5'-Hexynyl oligonucleotides synthesized in the previous section were used. Pullulan ($Mw = 1.0 \times 10^5$) was purchased from Hayashibara (Okayama, Japan). Superdehydrated dimethyl sulfoxide (DMSO), deoxidized DMSO, and t-butyl alcohol (t-BuOH) were obtained from Wako Pure Chemical (Osaka, Japan). Tris[(1-benzyl-1H-1,2,3-triazol-4-yl)methyl]amine (TBTA) and 3-azidopropylamine were obtained from Tokyo Chemical Industry (Tokyo, Japan). 1.1-Carboxyldiimidazole (CDI) and copper(I) bromide (CuBr) were obtained from Sigma–Aldrich (MO, USA). EDTA·3Na was obtained from Dojindo Laboratories (Kumamoto, Japan). All ^{1}H NMR spectra were recorded on a Bruker 400 MHz instrument.

Synthesis of azido-modified pullulan (pullulan-N_3)

Pullulan-N_3 was synthesized using a modified method reported previously [25]. Briefly, pullulan (1.00 g, 6.17×10^{-3} mol as glucose units) was dissolved in DMSO (60 mL) in a dry three-necked flask, to which CDI (0.200 g, 1.23×10^{-3} mol) was added. The reaction was carried out at 30 °C for 4 h. 3-Azidopropylamine (0.182 ml, 1.85×10^{-3} mol) was added dropwise, and the mixture was stirred at 30 °C for 24 h. The product was then purified by dialysis against distilled water for 4 days using a 3500 molecular weight cutoff dialysis membrane (Spectrum Laboratories, CA, USA) and then lyophilized to give a white solid. The degree of azide substitution in pullulan, which was 5.2 per 100 glucose units, was calculated by analyzing ^{1}H NMR spectra (DMSO-d_6/D_2O = 9/1 (v/v), 80 °C) (Fig. S1).

Synthesis of oligonucleotide-grafted pullulan by click chemistry

A mixture of pullulan-N_3 (4.0×10^{-2} g, 1.2×10^{-5} mol as azide groups) and 5'-hexynyl oligonucleotide (3.0×10^{-2} g, 1.4×10^{-5} mol) was dissolved in water and then deoxidized. Afterward, a solution of CuBr (4.3×10^{-3} g, 3.0×10^{-5} mol) and TBTA (3.2×10^{-2} g, 6.0×10^{-5} mol) dissolved in deoxidized DMSO/t-BuOH (11/1 (v/v), 4.5 mL) was added and stirred at 40 °C for 48 h. After cooling to room temperature

(RT), the reaction mixture was dialyzed against DMSO, EDTA-3Na solution, and distilled water using a dialysis membrane (molecular weight cutoff of 3500) and finally lyophilized to obtain the solid products. The degree of oligonucleotide substitution in pullulan-N_3 was calculated by analyzing ^{1}H NMR spectra (DMSO-d_6/D_2O = 9/1 (v/v), 80 °C).

Characteristics of oligonucleotide-grafted pullulan

Preparation of oligonucleotide-grafted pullulan nanogels

Oligonucleotide-grafted pullulan was dissolved in PBS at 25 °C with stirring to achieve a given concentration. These solutions were mixed fully to ensure that the molar concentrations of the oligonucleotides were equal. Nanogel solutions were then prepared by sonication (100 W, 28 Hz) in an ice water bath for 3 min.

Particle size and zeta potential analysis of the nanogels

The particle size and ζ-potential of oligonucleotide-grafted pullulan nanogels at various concentrations in PBS were measured with a Zetasizer Nano ZS (Malvern Instruments, Worcestershire, UK). The detector angles were 173° for the dynamic light scattering (DLS) measurements and 17° for the ζ-potential measurements. The measured autocorrelation function was analyzed using cumulant and nonnegative least squares analysis.

Transmission electron microscopy (TEM)

The prepared nanogel suspension (10 μL) was dropped onto elastic carbon-coated grids (#100, ELS-C10; Okenshoji, Japan) and allowed to stand at room temperature for 5 min. Samples were stained with 1% phosphotungstic acid solution for 5 min and observed using an HT7700 transmission electron microscope (Ibaraki, Japan) at an accelerating voltage of 100 kV.

Size-exclusion chromatography-multiangle light scattering

Size-exclusion chromatography combined with a multiangle light scattering (MALS) system consisted of a DP-8020 pump (Tosoh Co., Tokyo, Japan), an Optilab T-rEX refractive index (RI) detector (Wyatt Technology, Santa Barbara, CA, USA), and a Dawn Heleos II MALS detector with a 658-nm laser (Wyatt Technology, Santa Barbara, CA, USA). An SB-806 M HQ column (Showa Denko, Tokyo, Japan) was eluted with PBS (pH 7.4; Sigma–Aldrich) at a flow rate of 0.5 mL/min at 25–60 °C. The weight-average molecular weight (MW) based on the Rayleigh scattering equation was calculated using ASTRA VI software (Wyatt Technology) [26]. A RI increment (dn/dc) value of 0.142 mL/g of pullulan was used. The association number of oligonucleotide-grafted pullulan molecules per nanogel was calculated from the M_W of the nanogels. The average polymer density (Φ_H) of the nanogel was calculated from the experimental R_H and M_w values according to Eq. (1):

$$\Phi_{\mathrm{H}} = \left(\frac{M_W}{N_A}\right)\left(\frac{4}{3}\pi R_H^3\right)^{-1} \quad (1)$$

where N_A is Avogadro's number.

Evaluation of interactions between nanogels and oligonucleotide-grafted model molecules

Oligonucleotide-grafted pullulan (Pul-A**G**CC**G**A) was dissolved in 0.5 mg/mL PBS, and FAM-labeled oligonucleotides (GeneDesign Inc., Osaka, Japan) with complementary sequences were added to the Pul-A**G**CC**G**A solution at an oligonucleotide molar ratio of 5:1 (grafted to pullulan:FAM-labeled). FAM-TTTCGGCT, FAM-TTTC**GG**CT, FAM-TTT**CGG**CT, and FAM-TTT**CGGC**T were used as model molecules. Bold and underlined letters in the sequence notation indicate BNA. The mixture was annealed by reducing the temperature from 90 °C to 4 °C at a rate of 1 °C/min. Pul-TC**GG**CT (0.5 mg/mL) was then added, and FAM-labeled oligonucleotide-complexed nanogels were prepared by the procedure described above. The resulting complex dispersion was measured by DLS. To evaluate the formation of FAM-labeled oligonucleotide/nanogel complexes, agarose gel (4%) electrophoresis (25 V, 20 min) was performed at 37 °C in 40 mM Tris-acetate buffer (pH of 7.4).

Interaction of FAM-labeled oligonucleotide/nanogel complexes with cells

Mouse macrophage-like cells (Raw264.7) were seeded in 24-well plates at 1.0×10^5 cells/well and precultured in Dulbecco's modified Eagle's medium (DMEM) supplemented with 10% heat-inactivated fetal bovine serum for 24 h at 37 °C in 5% humidified CO_2. The FAM-TTT**CGGC**T/nanogel complex (100 μL) prepared in the previous section was mixed with 900 μL of DMEM, which was replaced with the medium of the precultured cells, and then cocultured for 12 h. The cells were then washed twice with PBS, detached, and dispersed with a scraper. Flow cytometry measurements were performed on a Cytomics FC500 (Beckman Coulter Inc., CA, USA) with a 488-nm argon laser. The signal from the FL1 bandpass emission (525 nm) was used for FAM.

Table 1 T_m values of oligonucleotides with self-complementary sequences (palindromic sequences)

Sequences	T_m (°C)	Sequences	T_m (°C)
GCGC	24 °C	GAGCTC	23 °C
GC**G**C	48 °C	GA**G**CTC	38 °C
AGGCCT	30 °C	**G**A**G**CTC	57 °C
AG**G**CCT	41 °C	GA**GC**TC	64 °C

Bold and underlined letters in the sequence indicate BNA

Results and discussion

T_m of BNA-modified oligonucleotides

In the design of oligonucleotide-grafted pullulan, 4- and 6-mer oligonucleotides (GeneDesign Inc., Osaka, Japan) with self-complementary sequences (palindromic sequences) were first used to study the effect of the number of BNA substituents on T_m. The oligonucleotides shown in Table 1 were dissolved in PBS solution (20 μM), and T_m was determined from temperature-controlled UV-absorbance measurements. T_m was less than 30 °C for both 4- and 6-mer nucleotides of the natural type, whereas T_m increased by more than 10 °C when one guanine nucleotide in the sequence was replaced with BNA. In addition, T_m dramatically increased when BNAs in the sequence formed base pairs with each other (GA**GC**TC). These results indicated that, as self-assembling units, oligonucleotides less than the 6-mer in length should contain two or more BNAs in their sequences to enable sufficient binding.

Synthesis of oligonucleotide-grafted pullulan

On the basis of the results in Table 1, we first designed an oligonucleotide-grafted pullulan that consisted of a 4-mer oligonucleotide with the BNA(**G**)-containing palindromic sequence **G**C**G**C. Specifically, oligonucleotide-grafted pullulan (Pul-**G**C**G**C) (Fig. 2) was synthesized by a click reaction between pullulan azide and an oligonucleotide with an alkyne at the 5' end, resulting in 2.8 **G**C**G**C molecules grafted per 100 monosaccharides (Fig. S2). We also selected a 6-mer oligonucleotide with a complementary nonpalindromic sequence and higher T_m to form stable duplexes, and we synthesized four different oligonucleotide-grafted pullulans with different numbers of BNA (**G** or **C**) replacements. Oligonucleotide-grafted pullulan (Pul-A**G**CC**G**A, Pul-A**GCCG**A, Pul-TC**GG**CT, and Pul-T**CGG**CT) was synthesized by introducing A**G**CC**G**A or A**GCCG**A and their complementary sequences of TC**GG**CT or T**CGG**CT into pullulan (Figs. S3–S6).

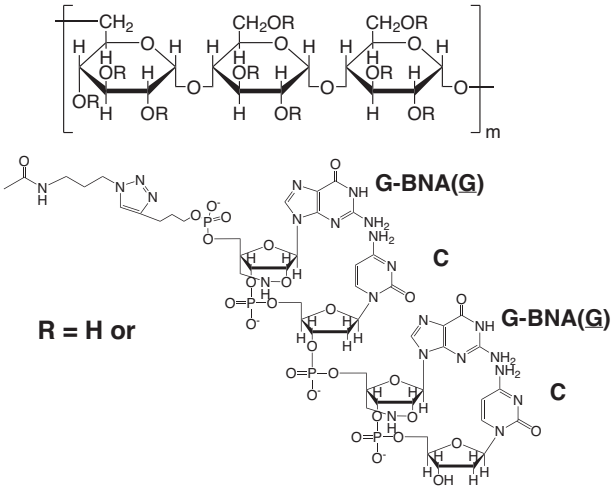

Fig. 2 Chemical structure of **G**C**G**C-grafted pullulan (Pul-**G**C**G**C)

Table 2 Characteristics of Pul-**G**C**G**C

	DS of Oligo (/100 glc)[a]	$N_{BNA\text{-}BNA}$	D_H (nm)	M_w	$N_{Pul\text{-}oligo}$
Pul-**G**C**G**C	2.8	0	30	1.2×10^5	1

Bold and underlined letters in the sequence indicate BNA

[a]Number of grafted moieties per 100 sugar units. DS of Oligo is the degree of substitution of oligonucleotides; $N_{BNA\text{-}BNA}$ is the number of base pairs formed between BNAs in oligonucleotide duplexes; D_H is the hydrodynamic radius; M_w is the weight-average molecular weight by SEC–MALS; $N_{Pul\text{-}oligo}$ is the aggregation number of Pul-oligo per nanoparticle

Self-assembly behavior of pullulan grafted with a 4-mer with a palindromic sequence

In the case of oligonucleotide double-strand formation as an associated force, two complementary sequences of oligonucleotides are generally employed. However, since oligonucleotides with palindromic sequences can form double strands on their own, we first investigated the potential for self-assembly in pullulan bearing a single type of oligonucleotide with a palindromic structure. As shown in Table 1, **G**C**G**C with a palindromic sequence had a T_m of 48 °C; thus, we expected Pul-**G**C**G**C to self-assemble through the formation of duplexes at temperatures above room temperature. Pul-**G**C**G**C was dissolved in PBS (1 mg/mL), sonicated, and characterized at 20 °C using DLS. The D_H was 30 ± 0.7 nm (Table 2). TEM images confirmed that the nanoparticles were 10–20 nm in size (Fig. 3B). However, the molecular weight (M_w) of the microparticles from SEC–MALS was 1.2×10^5, suggesting that the nanoparticles were formed by oligonucleotide duplex formation within the Pul-**G**C**G**C molecule, not between Pul-**G**C**G**C molecules (Table 2 and Fig. 3A).

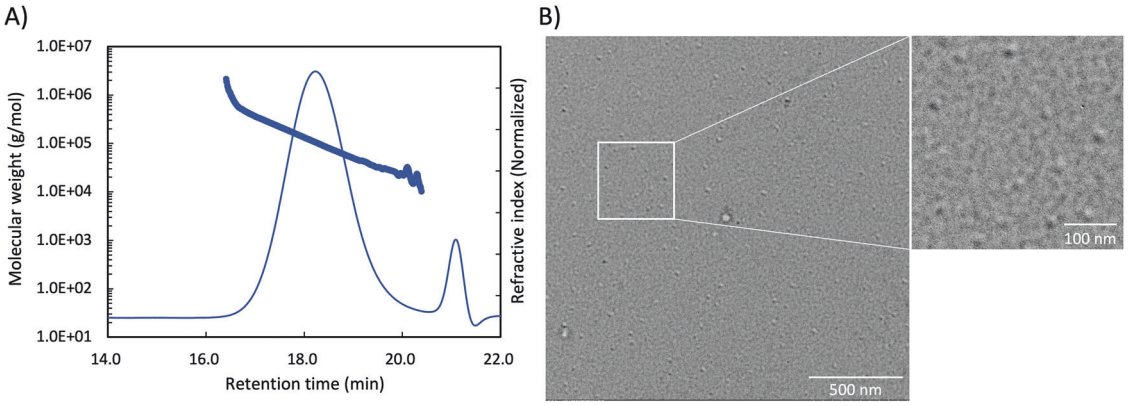

Fig. 3 **A** SEC–MALS chromatograms (RI intensity) at 25 °C to determine the molecular weight distribution of Pul-GCGC. **B** TEM image of Pul-GCGC in PBS

Self-assembly behavior of pullulans grafted with 6-mer nucleotides with complementary sequences

The self-assembly behavior of Pul-AGCCGA and Pul-TCGGCT was examined. The former contained the 6-mer oligonucleotide AGCCGA, with two BNA(G) replacements, introduced into pullulan at 2.4 oligonucleotides per 100 monosaccharides, whereas the latter contained a 6-mer oligonucleotide with the complementary sequence, TCGGCT, grafted onto pullulan at 2.1 oligonucleotides per 100 monosaccharides.

DLS measurements of Pul-AGCCGA (0.5 mg/mL) and Pul-TCGGCT (0.5 mg/mL) at 20 °C were used to determine their sizes: $D_H = 11 \pm 4$ nm (number distribution) for Pul-AGCCGA and $D_H = 16 \pm 4$ nm (number distribution) for Pul-TCGGCT. The two types of grafted pullulans were mixed at a volume ratio of 1:1 and sonicated (3 min). Subsequent DLS measurements confirmed the formation of nanoparticles with a $D_H = 91$ nm (polydispersity index, PDI = 0.23) (Fig. 4A and Table 3). The effect of concentration (final concentration after mixing) on nanoparticle size was examined, revealing that as the concentration increased, the size increased, but the PDI remained nearly the same at 0.20–0.25 (Fig. 4B). These results indicate that the particle size can be controlled by adjusting the concentration of pullulan in the mixture.

TEM images of the abovementioned self-assembled nanoparticles (final concentration: 0.5 mg/mL) revealed spherical structures approximately 100 nm in diameter (Fig. 4C). The M_w of the nanoparticles, as determined using SEC–MALS measurements, was 6.7×10^6 (Table 3). Calculating the number of associations between Pul-AGCCGA and Pul-TCGGCT in the nanoparticles with a theoretical molecular weight of 1.25×10^5 indicated that approximately 53 molecules of oligonucleotide-grafted pullulan self-assembled to form the nanoparticles. The density of the assembled nanoparticles, which was calculated by substituting the determined size (D_H) and molecular weight (M_w) into Eq. (1), was 0.028 g/mL, indicating that the hydrogel contained more than 90% water (Table 3).

To investigate duplex formation between oligonucleotides in the assembled nanoparticles, the T_m was calculated from temperature-controlled UV absorbance measurements. The T_m was 43 °C for the assembled nanoparticles consisting of Pul-AGCCGA and Pul-TCGGCT (Table 3 and Fig. S7), indicating that oligonucleotide duplex formation was also possible at 20 °C, the temperature under which assembly formation was evaluated. SEC–MALS measurements at 60 °C above the T_m of the assembled nanoparticles revealed that the number of associations decreased significantly from 53 (25 °C) to 1.8 (60 °C), indicating that above T_m, the oligonucleotide duplexes dissociated and the nanoparticles collapsed (Table 4 and Fig. S9). From these results, we concluded that mixtures of AGCCGA- and TCGGCT-grafted pullulans self-assemble into thermoresponsive nanogels through the formation of oligonucleotide duplexes, with these duplex sites serving as crosslinking points of the network.

Effect of the number of BNA substituents in oligonucleotides

Two BNA substituents exist in the oligonucleotides of Pul-AGCCGA and Pul-TCGGCT. Next, we increased the number of BNA substituents and investigated the self-assembly behavior between the resulting oligonucleotide-grafted pullulans. Three different mixtures were investigated: Pul-AGCCGA and Pul-TCGGCT, Pul-AGCCGA and Pul-TCGGCT, and Pul-AGCCGA and Pul-TCGGCT.

Table 3 shows the results of the DLS, SEC–MALS, and T_m measurements for each mixture. In all the systems, assembled nanoparticles formed at 20 °C (DLS) and 25 °C (SEC–MALS). As the number of base pair formations between BNAs in oligonucleotide duplexes ($N_{BNA\text{-}BNA}$)

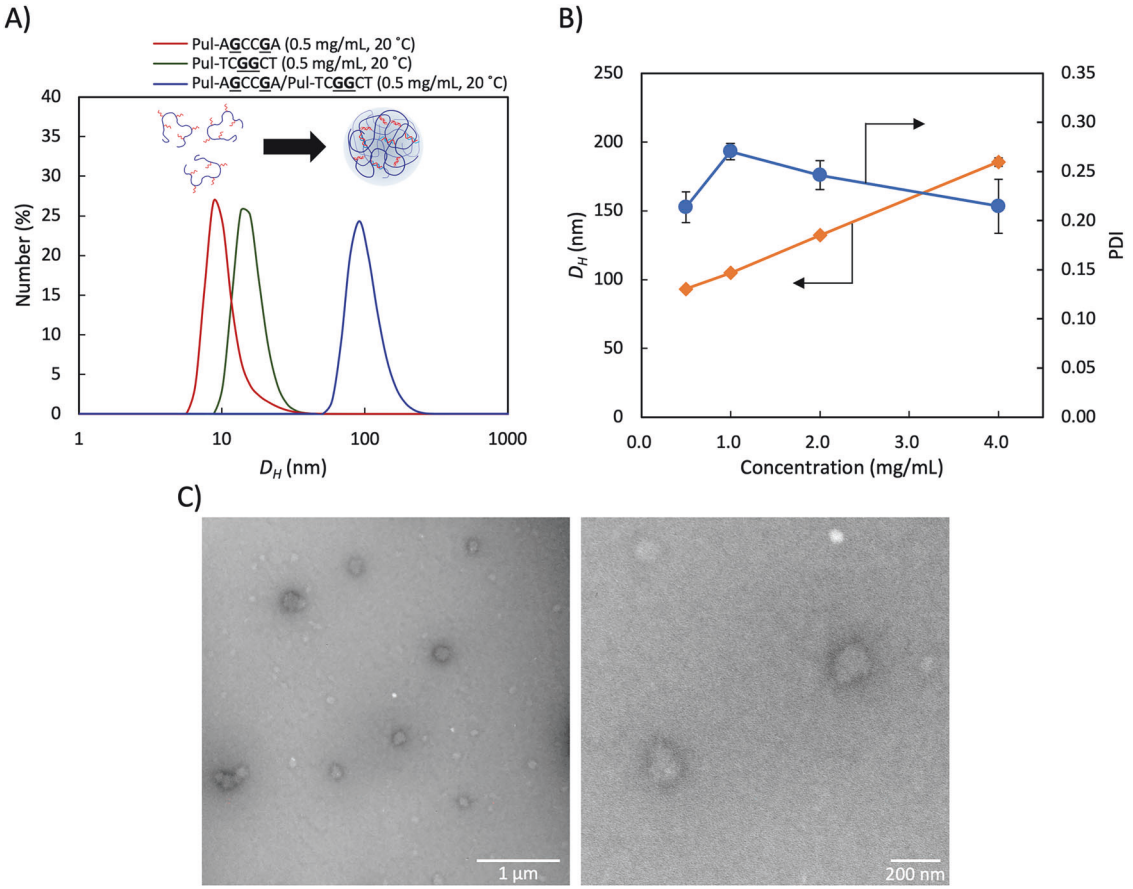

Fig. 4 **A** Changes in the size distribution of self-assembled Pul-AGCCGA/Pul-TCGGCT (0.5 mg/mL) in PBS at 20 °C, as measured by DLS. **B** Assembly of Pul-AGCCGA/Pul-TCGGCT at various concentrations (as equal oligonucleotide molar ratios) in PBS at 20 °C measured by DLS ($n = 3$, mean ± S.D.). **C** TEM image of Pul-AGCCGA/Pul-TCGGCT nanogels in PBS (0.5 mg/mL)

Table 3 Characteristics of 6-mer oligonucleotide-grafted pullulans

	DS of Oligo (/100 glc)[a]	$N_{BNA\text{-}BNA}$	T_m	D_H (nm)	Z potential (mV)	M_w	$N_{Pul\text{-}oligo}$	Φ_H (g/mL)
Pul-AGCCGA/ Pul-TCGGCT	2.4 2.1	0	43	91	–6.9	6.7×10^6	53	0.028
Pul-AGCCGA/ Pul-TCGGCT	2.4 2.1	1	52	73	–8.5	5.1×10^6	41	0.042
Pul-AGCCGA/ Pul-TCGGCT	3.0 2.1	2	65	60	–4.8	3.9×10^6	31	0.057
Pul-AGCCGA/ Pul-TCGGCT	3.0 2.1	3	78	51	–9.6	3.1×10^6	25	0.074

Bold and underlined letters in the sequence indicate BNA

[a]Number of grafted moieties per 100 sugar units. DS of Oligo is the degree of substitution of oligonucleotides; $N_{BNA\text{-}BNA}$ is the number of base pairs formed between BNAs in oligonucleotide duplexes; T_m is the melting temperature from UV-absorbance measurements; D_H is the hydrodynamic diameter at 20 °C; M_w is the weight-average molecular weight at 25 °C by SEC–MALS; $N_{Pul\text{-}oligo}$ is the aggregation number of Pul-oligo per nanoparticle; Φ_H is the average polymer density

increased, the particle size (D_H) decreased, and the density of the nanogel increased. The T_m increased significantly (more than 10 °C) as the number of BNA–BNA pairs increased by one. Moreover, the temperature response of the nanogel could be controlled by adjusting the number of BNA substituents in the oligonucleotides. Furthermore, SEC–MALS measurements of the nanogels at various temperatures confirmed that the number of associations decreased at temperatures near the T_m, indicating that the nanogels disintegrated (Table 4).

Complexation of nanogels and model drug molecules using duplex formation of oligonucleotides and their interaction with cells

By conjugating various drugs or tags to BNA-containing oligonucleotides and then complexing these drug/tag-conjugated oligonucleotides with oligonucleotide-grafted pullulans, the complexed nanogels can be applied as nanocarriers. In this experiment, 6-carboxyfluorescein (FAM), a fluorescent molecule, was selected as a model drug/tag molecule, and oligonucleotides with various numbers of BNAs (FAM-oligo) were modified with FAM at the 5' end to evaluate complex formation with the nanogels.

Table 4 Effect of temperature on the self-assembly of 6-mer oligonucleotide-grafted pullulans

	$N_{BNA\text{-}BNA}$	$N_{Pul\text{-}oligo}$			
		25 °C	40 °C	50 °C	60 °C
Pul-A**G**CC**G**A/ Pul-TCGGCT	0	53	3.6	1.8	1.8
Pul-A**G**CC**G**A/ Pul-T**C**GG**C**T	1	41	65	5.7	2.0
Pul-A**GCCG**A/ Pul-TC**GG**CT	2	31	27	34	10
Pul-A**GCCG**A/ Pul-T**CGGC**T	3	25	28	25	39

Bold and underlined letters in the sequence indicate BNA. $N_{BNA\text{-}BNA}$ is the number of base pairs formed between BNAs in oligonucleotide duplexes; $N_{Pul\text{-}oligo}$ is the aggregation number of Pul-oligo per nanoparticle, calculated using M_w determined with SEC–MALS

First, we examined the formation of complexes under various molar ratios for the complementary oligonucleotide pair Pul-A**G**CC**G**A and FAM-TTTC**GG**CT, whose lowest *Tm* values are shown in Table 3. We set the molar ratio for these experiments to 5:1 because the formation of Pul-A**G**CC**G**A and FAM-TTTC**GG**CT complexes was incomplete at a molar ratio of 4:1 or lower (see Fig. S10). Pul-A**G**CC**G**A and Pul-TC**GG**CT were used as oligonucleotide-grafted pullulans. FAM-oligos (FAM-TTTCGGCT, FAM-TTTC**GG**CT, FAM-TTT**CGG**CT, and FAM-TTT**CGGC**T) were added to Pul-A**G**CC**G**A/PBS (0.5 mg/mL) at an oligonucleotide molar ratio of 5:1 (Pul-A**G**CC**G**A:FAM-oligo). The temperature of the mixture was increased to 90 °C and then cooled to 4 °C for annealing. Afterward, Pul-T**C**GG**C**T, with the complementary sequence, was added, and the resulting nanogels were prepared as described above (Fig. 5A). DLS measurements of each sample indicated that 70–90 nm nanoparticles formed in all the samples (Fig. 5B).

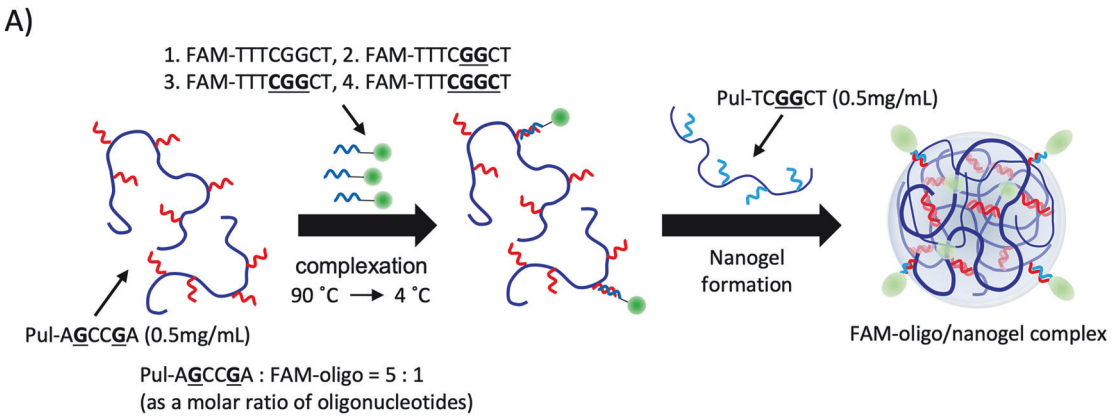

B)

Pul-oligo	FAM-oligo	D_H (nm)	PDI
Pul-A**G**CC**G**A/ Pul-TC**GG**CT	FAM-TTTCGGCT	91	0.33
	FAM-TTTC**GG**CT	73	0.37
	FAM-TTT**CGG**CT	73	0.28
	FAM-TTT**CGGC**T	69	0.26

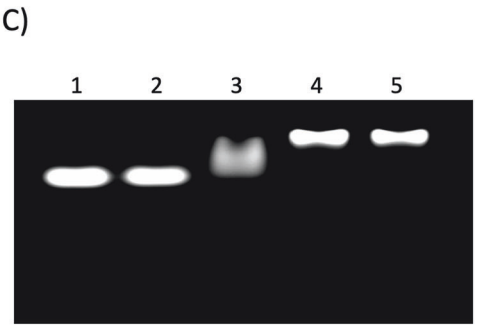

Fig. 5 **A** Preparation of FAM-oligo/nanogel complexes. **B** D_H of the FAM-oligo/nanogel complexes (D_H is the hydrodynamic diameter, and PDI is the polydispersity index). **C** Evaluation of FAM-oligo/nanogel complex formation by agarose gel (4.0%) electrophoresis with 40 mM Tris-acetate buffer (pH of 7.4) containing 1 mM EDTA at 25 V for 20 min at 37 °C. Lane 1: FAM-TTTCGGCT only, Lane 2: Nanogel/FAM-TTTCGGCT mixture, Lane 3: Nanogel/FAM-TTTC**GG**CT mixture, Lane 4: Nanogel/FAM-TTT**CGG**CT mixture, Lane 5: Nanogel/FAM-TTT**CGGC**T mixture

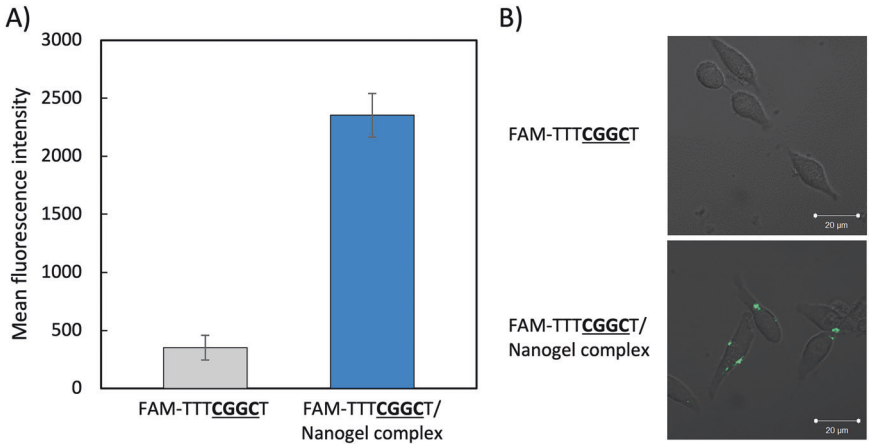

Fig. 6 Interaction between FAM-TTT**CGGC**T/Nanogel complexes and Raw 264.7 cells after 12 h. **A** Mean fluorescence intensity of cells treated with FAM-TTT**CGGC**T-complexed nanogels, as determined by flow cytometry ($n = 3$, mean ± SD). **B** CLSFM images of cells coincubated with FAM-TTT**CGGC**T-complexed nanogels after 12 h

Complexation of the nanogels with FAM-oligos was evaluated using agarose gel electrophoresis. The results revealed that FAM-TTT**CGG**CT and FAM-TTT**CGGC**T with three and four BNAs, respectively, were fully complex (Fig. 5C, Lanes 4 and 5) because free FAM-oligos were absent (Fig. 5C, Lane 1). Under these conditions, approximately 20 mol% of the oligonucleotides of Pul-A**G**CC**G**A complexed with FAM-oligo, and the remaining oligonucleotides of Pul-A**G**CC**G**A interacted with Pul-TC**GG**CT to cross-link the nanogel. The amount of FAM-oligo loaded in a single nanogel particle ranged from 50–80 molecules. Therefore, to promote stable complexation with the nanogels, drugs or functional groups should be conjugated to oligonucleotides containing multiple BNAs.

Finally, the interactions of drug-conjugated nanogels with cells were investigated. FAM-TTT**CGGC**T/nanogels (Pul-A**G**CC**G**A and Pul-TC**GG**CT) were added to precultured Raw264.7 cells and cocultured for 12 h, after which flow cytometry measurements were performed. With only FAM-TTT**CGGC**T, interactions with cells were not observed. In contrast, the cellular uptake of FAM-TTT**CGGC**T in complex with the nanogels significantly increased (Fig. 6). This increased cellular uptake of FAM-oligo complexed with nanogels was observed because macrophage phagocytosis of nanoparticles was effective and interactions between the oligonucleotides of the nanogels and nucleic acid receptors, such as Toll-like receptors, were strong [27, 28].

Conclusion

This study indicates that nanogels based on oligonucleotide-grafted pullulans are useful as carriers for intracellular delivery. By conjugating various functional units to BNA-containing oligonucleotides (e.g., bioactive proteins, functional nucleic acids, and targeting molecules), nanogels can be developed as new tailor-made nanocarriers for various bioapplications.

Acknowledgements The authors would like to thank M. Ando for useful advice on oligonucleotide synthesis. This work was supported by JSPS KAKENHI Grant Number JP18K12077, JP22H00585 and the Japan Agency for Medical Research and Development (243fa727001h0003). We thank Edanz (https://jp.edanz.com/ac) for editing a draft of this manuscript.

Compliance with ethical standards

Conflict of interest The authors declare no competing interests.

Publisher's note Springer Nature remains neutral with regard to jurisdictional claims in published maps and institutional affiliations.

References

1. Verduzco R, Li X, Pesek SL, Stein GE. Structure, function, self-assembly, and applications of bottlebrush copolymers. Chem Soc Rev. 2015;44:2405–20.
2. Wang A, Shi W, Huang J, Yan Y. Adaptive soft molecular self-assemblies. Soft Matter. 2016;12:337–57.

3. Ariga A, Nishikawa M, Mori T, Takeya J, Shrestha LK, Hill JP. Self-assembly as a key player for materials nanoarchitectonics. Sci Technol Adv Mater. 2019;20:51–95.
4. Chiriac AP, Ghilan A, Neamtu I, Nita LE, Rusu AG, Chiriac VM. Advancement in the biomedical applications of the (nano)gel structures based on particular polysaccharides. Macromol Biosci. 2019;19:1900187.
5. Yin Y, Hu B, Yuan X, Cai L, Gao H, Yang Q. Nanogel: a versatile nanodelivery system for biomedical applications. Pharmaceutics. 2020;12:290.
6. Ma X, Li SJ, Liu Y, Zhang T, Xue TP, Kang Y, et al. Bioengineered nanogels for cancer immunotherapy. Chem Soc Rev. 2022;51:5136–74.
7. Sasaki Y, Akiyoshi K. Nanogel engineering for new nanobiomaterials: from chaperoning engineering to biomedical applications. Chem Rec. 2010;10:366–76.
8. Tahara Y, Akiyoshi K. Current advances in self-assembled nanogel delivery systems for immunotherapy. Adv Drug Deliv Rev. 2015;95:65–76.
9. Muraoka D, Harada N, Shiku H, Akiyoshi K. Self-assembled polysaccharide nanogel delivery system for overcoming tumor immune resistance. J Control Release. 2022;347:175–82.
10. Papagiannopoulos A, Sotiropoulos K. Current advances of polysaccharide-based nanogels and microgels in food and biomedical sciences. Polymers. 2022;14:813.
11. Hajebi S, Rabiee N, Bagherzadeh M, Ahmadi S, Rabiee M, Roghani-Mamaqani H, et al. Stimulus-responsive polymeric nanogels as smart drug delivery systems. Acta Biomater. 2019;92:1–18.
12. Shu T, Hu L, Hunter H, Balasuriya N, Fang C, Zhang Q, et al. Multi-responsive micro/nanogels for optical sensing. Adv Phys-X. 2022;7. 2043185.
13. Cho H, Jeon S, Yang J, Baek SY, Kim D. Hydrogel nanoparticle as a functional coating layer in biosensing, tissue engineering, and drug delivery. Coatings. 2020;10:663.
14. Preman NK, Barki RR, Vijayan A, Sanjeeva SG, Johnson RP. Recent developments in stimuli-responsive polymer nanogels for drug delivery and diagnostics: a review. Eur J Pharm Biopharm. 2020;157:121–53.
15. Ma X, Li SJ, Liu Y, Zhang T, Xue P, Kang Y, et al. Bioengineered nanogels for cancer immunotherapy. Chem Soc Rev. 2022;51:5136–74.
16. Yang D, Zhou C, Gao F, Wang P, Ke Y. DNA-guided assembly of molecules, materials, and cells. Adv Intell Syst. 2020;2:1900101.
17. Gačanin J, Synatschke CV, Wei T. Biomedical applications of DNA-based hydrogels. Adv Funct Mater. 2020;30:1906253.
18. Iqbal S, Ahmed F, Xiong H. Responsive-DNA hydrogel-based intelligent materials: preparation and applications. Chem Eng J. 2021;420:130384.
19. Iwasaki Y, Kondo J, Kuzuya A, Moriyama R. Crosslinked duplex DNA nanogels that target specified proteins. Sci Technol Adv Mater. 2016;17:285–92.
20. Ding F, Mou Q, Ma Y, Pan G, Guo Y, Tong G, et al. A crosslinked nucleic acid nanogel for effective siRNA delivery and antitumor therapy. Angew Chem Int Ed. 2018;57:3064–68.
21. Murakami Y, Maeda M. Hybrid hydrogels to which single-stranded (ss) DNA probe is incorporated can recognize specific ssDNA. Macromolecules. 2005;38:1535–37.
22. Peng L, You M, Yuan Q, Wu C, Han D, Chen Y, et al. Macroscopic volume change of dynamic hydrogels induced by reversible DNA hybridization. J Am Chem Soc. 2012;134:12302–07.
23. Rahman SMA, Seki S, Obika S, Yoshikawa H, Miyashita K, Imanishi T. Design, synthesis, and properties of 2',4'-BNA(NC): a bridged nucleic acid analogue. J Am Chem Soc. 2008;130:4886–96.
24. Rahman SMA, Imanishi T, Obika S. Synthesis of several types of bridged nucleic acids. Chem Lett. 2009;38:512–17.
25. Morimoto N, Hirano S, Takahashi H, Loethen S, Thompson DH, Akiyoshi K. Self-assembled pH-sensitive cholesteryl pullulan nanogel as a protein delivery vehicle. Biomacromolecules. 2013;14:56–63.
26. Wyatt PJ. Light scattering and the absolute characterization of macromolecules. Anal Chim Acta. 1993;272:1–40.
27. Mosquera J, García I, Liz-Marzán LM. Cellular uptake of nanoparticles versus small molecules: a matter of size. Acc Chem Res. 2018;51:2305–13.
28. Maeda M, Kojima T, Song Y, Takayama S. DNA-based biomaterials for immunoengineering. Adv Health Mater. 2019;8:1801243.